On Damping Created by the Heterogeneity of the Mechanical Properties in RC Frame Seismic Analysis

P. Jehel & R. Cottereau
Laboratoire MSSMat (UMR 8579), École Centrale Paris, CNRS
Grande Voie des Vignes, 92295 Châtenay-Malabry Cedex, France
e-mail: pierre.jehel[at]ecp.fr

SUMMARY:
In the dynamic analysis of structural engineering systems, it is common practice to introduce additional damping models to reproduce some of the features observed experimentally. We report here on a preliminary work towards an alternative path for material damping, that aims at reproducing these features through the consideration only of the heterogeneous character of the yield stress field. The heterogeneity is parameterized by a stochastic model, controlled by three parameters only: a mean value, a variance parameter and a correlation length. For a single-degree-of-freedom elasto-plastic system with linear kinematic hardening, we show that such a variability indeed creates the patterns that are classically associated to viscous damping, and that would otherwise be modeled through nonlinear hardening, local hysteresis loops or other such complex constitutive models. A quasi-static force-displacement experiment and the dynamic bending response of a cantilever beam are presented as illustration.

Keywords: Damping, reinforced concrete, fiber beam element, stochastic inelastic constitutive law, material heterogeneity.

1. INTRODUCTION

1.1. Motivations

Within the last few decades, a great deal of attention was paid to the comprehension and modeling of damping mechanisms in inelastic time-history analyses. For instance, these questions occupy an important share of the latest reports on seismic design (PEER/ATC-72-1 October 2010, section 2.4). The common practice consists in simply adding a damping model to the inelastic structural model, to reproduce the phenomena observed experimentally. However, the choices of damping model and parameters are not necessarily founded on a rational basis. In particular, the widely used Rayleigh damping is well known to lack physical background, even when care is taken to avoid spurious damping forces (Charney 2008, Hall 2006).

We try in this paper to circumvent the need to introduce these non physically-based damping models by observing that the relevant experimental observations can be equally well explained by the simple introduction of spatial variability in the parameters of the inelastic structural model. In particular, we will report here on observations of damping arising from the consideration of the spatial fluctuations of the yield stress in an inelastic reinforced (RC) concrete frame element. This heterogeneity will be introduced through a stochastic model of the mechanical properties and both a quasi-static force-displacement experiment and the dynamic bending response of a cantilever beam will be investigated. Special attention will be devoted to the capability of the model for dissipating energy even for low-amplitude loadings, which is a key issue for earthquake engineering applications.

1.2. Modeling concrete in fiber frame elements

A numerical representation of the mesoscopic structure of concrete has been developed using a spatial truss model and is capable of representing the salient characteristics of concrete in uni- and multi-axial loading conditions (Benkemoun et al. 2010). Because such a model is very demanding from a computa-

tional point of view, it is not realistic to use it for structural engineering applications. In RC fiber frame element model, each beam (column) control section is divided into fibers that represent either concrete or steel, with the appropriate uniaxial behavior law. The computation is thus rendered more efficient.

In (Jehel et al. 2010), a concrete constitutive law is developed in the framework of *thermodynamics with internal variables* (Maugin 1999). It is capable of representing, for the compression part: viscoelastic behavior, permanent deformation, loss of stiffness, strain hardening and softening, local hysteresis loops, and for the tension part: elastic brittle response. All these phenomena are necessary to properly represent the inelastic response – the energy dissipative phenomena that contribute to the overall structural damping – of a concrete block in uniaxial cyclic loading. For a given material, it is generally taken for granted that the same behavior law can be assigned to every numerical integration point (fiber centroids in the beam control sections).

1.3. Stochastic heterogeneous model

Several authors in structural engineering literature have already considered stochastic heterogeneous models of the mechanical parameters. Indeed, those are often used in order to take into account the uncertainty in the parameters and their influence on mechanical behavior. In (Stefanou & Fragiadakis 2009), steel frames with spatially varying Young's modulus and yield stress are generated and the propagation of this initial heterogeneity on the structural dynamic inelastic response is investigated through Monte Carlo simulations (MCS). In (Real et al. 2003), uncertain material and geometrical properties are considered in the analysis of a 2D reinforced concrete beam. The concrete finite element mesh is composed of 2D plane stress elements with three constitutive parameters, which vary at each numerical integration point according to the fluctuations of three correlated 2D Gaussian random fields. Steel rebars are introduced as rigid lines in concrete elements and with material uncertainty too. Variability of the beam height is also introduced. MCS techniques are used to measure the induced uncertainty on the structural response. Material and geometrical variability in RC frame structures are also considered in (Lee & Mosalam 2004). The authors develop a stochastic finite element method based on a beam element that combines both the fiber beam formulation and the midpoint method for random field representation. MCS are performed with material variability in both concrete and steel, and in both the beam cross section and along its length; geometric variability is also considered.

Although the present paper will make use of the same type of stochastic models as the authors above, it should be stressed that the objective here is altogether different. In the literature, the objective is to represent the influence of uncertainty using many realizations of the random medium, along with statistical analysis (averages of the solution, variance, *etc*). Our objective, here, is to observe on each single realization of the random medium, the influence of the heterogeneity, in particular with a view at experimental features that are more classically taken into account today through damping models. There is hence no statistical analysis involved, once a realization of the random model of mechanical parameters has been drawn.

1.4. Outline

In the following section, we recall the theoretical formulation of the inelastic fiber frame element that will then be used for numerical applications. In section 3, the uniaxial stochastic local constitutive model to be assigned to every concrete fiber is presented. It is an elasto-plastic law with linear kinematic hardening and spatially variable yield stress. This model has to convey the heterogeneous nature of concrete at the fiber scale, relying on the fluctuations of a lognormal random field with a correlation length defined in accordance with the size of the aggregates in concrete. The last section is dedicated to numerical applications.

2. FIBER BEAM ELEMENT FORMULATION FOR SEISMIC ANALYSIS

In this section, we recall the theoretical basis for the displacement-based formulation of a fiber beam element with Euler-Bernoulli kinematics assumption. Nevertheless, note that force-based and mixed formulations exist (Taylor et al. 2003) and that, in (Stefanou & Fragiadakis 2009), it is claimed that the mixed formulation used offers significant computational advantages for the analysis of systems with

stochastic properties, compared to the classical displacement-based formulation.

2.1. Continuum Euler-Bernoulli beam

We consider a 2D continuum $\Omega \subset \mathbb{R}^2$ with frontier $\partial\Omega$ constrained to the displacement $\mathbf{u}^{ext}(t)$ on the portion $\partial\Omega_u$ and to the external pressure $\mathbf{f}_s(t)$ on $\partial\Omega_\sigma$. Besides, we set $\partial\Omega = \partial\Omega_u \cup \partial\Omega_\sigma$ and $\partial\Omega_u \cap \partial\Omega_\sigma = \varnothing$. We denote $(\mathbf{e}_1, \mathbf{e}_2)$ a cartesian basis of $\mathbb{R}^2$ so that $\mathbf{x} = x_1\mathbf{e}_1 + x_2\mathbf{e}_2$ and $\mathcal{U} = \{\mathbf{u}(\mathbf{x},t) : \Omega \times [0,T] \mapsto \mathbb{R}^2 \mid \forall \mathbf{x} \in \partial\Omega_u,\ \mathbf{u}(\mathbf{x},t) = \mathbf{u}^{ext}(t)\ ;\ \mathbf{u}(\mathbf{x},0) = \mathbf{u}_0(\mathbf{x})\ ;\ \dot{\mathbf{u}}(\mathbf{x},0) = \dot{\mathbf{u}}_0(\mathbf{x})\}$.

The so-called Euler-Bernoulli kinematics assumption for a displacement field $\mathbf{u}(\mathbf{x},t) \in \mathcal{U}$ can be written:

$$\mathbf{u}(\mathbf{x},t) = \begin{pmatrix} u_1(\mathbf{x},t) = u_1^S(x_1,t) - x_2\theta_3^S(x_1,t) \\ u_2(\mathbf{x},t) = u_2^S(x_1,t) \end{pmatrix} \quad \text{with} \quad \theta_3^S(x_1,t) = \frac{\partial u_2^S(x_1,t)}{\partial x_1} \tag{1}$$

With the hypothesis of small transformations, the strain tensor reads:

$$\boldsymbol{\epsilon}(\mathbf{x},t) = \frac{1}{2}\left(\mathbf{D}(\mathbf{u}) + \mathbf{D}(\mathbf{u})^T\right) \tag{2}$$

where $\mathbf{D}(\cdot) = \frac{\partial \cdot}{\partial x_i} \otimes \mathbf{e}_i$ is the vector gradient operator.

We express the material constitutive behavior law as the following relation between the stress and strain fields:

$$\boldsymbol{\sigma}(\boldsymbol{\epsilon}) = \frac{\partial \psi(\boldsymbol{\epsilon})}{\partial \boldsymbol{\epsilon}}\ , \qquad \forall \mathbf{x} \in \Omega,\ \forall t \in [0,T] \tag{3}$$

where $\boldsymbol{\sigma} \in \mathcal{S} = \{\boldsymbol{\sigma}(\mathbf{x},t) : \Omega \times [0,T] \mapsto \mathbb{R}^2 \mid \forall \mathbf{x} \in \partial\Omega_\sigma, \boldsymbol{\sigma}\cdot\mathbf{n}(\mathbf{x}) = \mathbf{f}_s(\mathbf{x},t)\}$, with $\mathbf{n}(\mathbf{x})$ the unit vector orthogonal to $\partial\Omega$ and oriented toward the exterior of Ω. $\psi(\boldsymbol{\epsilon})$ is the stored energy function.

The problem of the dynamic evolution of a beam for earthquake engineering applications can then be set as:
Given the external forces $\mathbf{f}_s(\mathbf{x},t)$ and $\mathbf{f}_v(\mathbf{x},t)$, and the ground motion – supposed to be the same at each point of the base of the structure – $\mathbf{u}_g(t)$, find $\mathbf{u}(\mathbf{x},t) \in \mathcal{U}$ and $\boldsymbol{\sigma}(\mathbf{x},t) \in \mathcal{S}$, such that:

$$\int_\Omega \left(\mathbf{Div}\boldsymbol{\sigma} + \mathbf{f}_v - \rho\left(\ddot{\mathbf{u}}_g + \ddot{\mathbf{u}}\right)\right) \cdot \delta\mathbf{u}\ d\Omega = 0\ , \quad \forall \delta\mathbf{u} \in \mathcal{U}_0 \tag{4}$$

where $\mathcal{U}_0 = \{\delta\mathbf{u} : \Omega \times [0,T] \mapsto \mathbb{R}^2 \mid \forall \mathbf{x} \in \partial\Omega_u,\ \delta\mathbf{u}(\mathbf{x},t) = \mathbf{0}\}$ and $\mathbf{u}(\mathbf{x},t)$ is the displacement field of the structure in the moving frame attached to the ground.

Using the relation $\mathbf{Div}\boldsymbol{\sigma}\cdot\delta\mathbf{u} = div(\boldsymbol{\sigma}\cdot\delta\mathbf{u}) - \boldsymbol{\sigma} : \mathbf{D}(\delta\mathbf{u})$ and after integration by parts:

$$\int_\Omega \rho\ddot{\mathbf{u}}\cdot\delta\mathbf{u}\ d\Omega + \int_\Omega \boldsymbol{\sigma} : \mathbf{D}(\delta\mathbf{u})\ d\Omega = \int_\Omega \mathbf{f}_v\cdot\delta\mathbf{u}\ d\Omega + \int_{\partial\Omega} \mathbf{f}_s\cdot\delta\mathbf{u}\ d\partial\Omega - \int_\Omega \rho\ddot{\mathbf{u}}_g\cdot\delta\mathbf{u}\ d\Omega \tag{5}$$

Introducing the Euler-Bernoulli kinematic assumption, we have:

$$\delta\mathbf{u} = \begin{pmatrix} \delta u_1^S(x_1,t) - x_2\delta\frac{\partial u_2^S(x_1,t)}{\partial x_1} \\ \delta u_2^S(x_1,t) \end{pmatrix} \tag{6}$$

leading to the following expression of the internal energy term:

$$\int_\Omega \boldsymbol{\sigma} : \mathbf{D}(\delta\mathbf{u})\ d\Omega = \int_L \left\{ \int_{S(x_1)} \sigma_{11}\left(\frac{\partial\delta u_1^S}{\partial x_1} - x_2\frac{\partial^2\delta u_2^S}{\partial x_1^2}\right) dS(x_1)\right\} dx_1 \tag{7}$$

2.2. Fiber tangent modulus

Beam sections are divided into fibers according to the following relation:

$$\int_{S(x_1)} h(\mathbf{x}^f,t)dS(x_1) \approx \sum_{f=1}^{n_{fib}} A^f(x_1)h(\mathbf{x}^f,t) \qquad \text{with} \qquad \mathbf{x}^f = x_1\mathbf{e}_1 + x_2^f\mathbf{e}_2 \tag{8}$$

where $A^f(x_1)$ is the section area and x_2^f is the position of the centroid of the fiber f in the beam section $S(x_1)$.

To any displacement evolution $\mathbf{u}(\mathbf{x},t+\Delta t) = \mathbf{u}(\mathbf{x},t) + \Delta\mathbf{u}(\mathbf{x},t)$ is associated a strain increment $\Delta\boldsymbol{\epsilon}(\mathbf{x},t)$. Assuming linear evolution of the stress field with respect to the strain field during time step Δt, and uniaxial inelastic behavior law $\sigma_{11} = \sigma_{11}(\epsilon_{11})$, we have the following expression:

$$\int_\Omega \boldsymbol{\sigma}(\boldsymbol{\epsilon}+\Delta\boldsymbol{\epsilon}) : \mathbf{D}(\delta\mathbf{u})\, d\Omega = \int_\Omega \boldsymbol{\sigma}(\boldsymbol{\epsilon}) : \mathbf{D}(\delta\mathbf{u})\, d\Omega + \int_L \sum_{f=1}^{n_{fib}} A^f \frac{d\sigma_{11}^f}{d\epsilon_{11}^f}\Delta\epsilon_{11}^f \left(\frac{\partial\delta u_1^S}{\partial x_1} - x_2^f\frac{\partial^2\delta u_2^S}{\partial x_1^2}\right) dx_1 \tag{9}$$

where $C_{11}^f = \frac{d\sigma_{11}^f}{d\epsilon_{11}^f}$ is the tangent modulus associated to the uniaxial material constitutive law of fiber f. For reinforced concrete beams, this corresponds to either concrete or steel pointwise constitutive response.

In the next section, we derive the equations for computing the tangent modulus and the uniaxial stress in every beam fibers. For the sake of conciseness, we set $C = C_{11}^f$ and $\sigma = \sigma_{11}^f$.

3. STOCHASTIC ELASTO-PLASTIC CONSTITUTIVE MODEL

As first investigation, the local material constitutive response at each fiber centroid is modeled by a uniaxial elasto-plastic law with linear kinematic hardening, and spatial variability is introduced by considering heterogeneous yield stress.

The three ingredients for an elasto-plastic material constitutive law developed in the framework of thermodynamics with internal variables (Maugin 1999) are i) the split of the total deformation into an elastic and a plastic part, ii) a stored energy function ψ, and iii) a yield criterium function $\tilde{\phi}$:

$$\epsilon = \epsilon^e + \epsilon^p \tag{10}$$

$$\psi(\epsilon^e,\lambda) = \psi^e(\epsilon^e) + \Lambda^p(\lambda) \quad \text{with} \quad \psi^e = \frac{1}{2}\epsilon^e E\epsilon^e \quad \text{and} \quad \Lambda^p = \frac{1}{2}\lambda H\lambda \tag{11}$$

$$\tilde{\phi}(\sigma) \leq 0 \tag{12}$$

We introduce spatial variability in the material behavior by introducing the fluctuations of a random field $f_0(\mathbf{x})$ in the criteria function:

$$\phi(\sigma,\kappa) = |\sigma+\kappa| - f_0(\mathbf{x})\sigma_y \tag{13}$$

where κ is the so-called back-stress and σ_y the mean yield stress. In this paper, $f_0(\mathbf{x})$ is modeled as a lognormal distribution function with mean $\mu = 1$, variance τ, and triangular power spectrum with correlation length $\ell_c = 1$ cm. As we only aim here at reporting first investigations on the influence of the variability of the yield stress on damping-like behavior of beams, we will not further discuss this choice. However, for example using the Maximum Entropy Principle (Shannon 1948, Jaynes 1957), it may be possible to propose random models more adapted for this specific mechanical parameter (see (Soize 2006, Cottereau et al. 2008, Ta et al. 2010) for examples of this type of approach in the linear elastic case).

The mechanical dissipation due to inelastic evolution of the system is defined as:

$$\dot{\mathcal{D}} = \sigma\dot{\epsilon} - \dot{\psi} = \left(\sigma - \frac{d\psi^e}{d\epsilon^e}\right)\dot{\epsilon}^e + \sigma\dot{\epsilon}^p + \kappa\dot{\lambda} \tag{14}$$

where $\kappa = -\frac{d\Lambda^p}{d\lambda} = -H\lambda$. During elastic evolution, the internal variables are frozen and material dissipation is null:

$$\left(\sigma - \frac{d\psi^e}{d\epsilon^e}\right)\dot{\epsilon}^e = 0 \qquad \Rightarrow \qquad \sigma = \frac{d\psi^e}{d\epsilon^e} = E\epsilon^e \tag{15}$$

$$\Rightarrow \qquad \dot{\mathcal{D}} = \sigma\dot{\epsilon}^p + \kappa\dot{\lambda} \tag{16}$$

The evolution of the interval variables is driven by appealing to the principle of maximum plastic dissipation which states that among all the dual variables sets $(\sigma^\star, \kappa^\star)$ satisfying $\phi(\sigma^\star, \kappa^\star) \leq 0$, the actual one maximizes $\dot{\mathcal{D}}$. Rewriting this maximization problem as the minimization of $-\dot{\mathcal{D}}$ under the constraint $\phi \leq 0$ and with non-negative plastic multiplier $\dot{\gamma}$, the Lagrange multiplier method is used (Strang 1986):

$$(\sigma, \kappa, \dot{\gamma}) = \underset{\phi^\star \leq 0; \dot{\gamma}^\star > 0}{\operatorname{argmin}} \; L \qquad \text{with} \quad L = \left(-\dot{\mathcal{D}}(\sigma^\star, \kappa^\star) + \dot{\gamma}^\star\phi(\sigma^\star, \kappa^\star)\right) \tag{17}$$

The solution of this problem is:

$$\frac{\partial L}{\partial \sigma^\star}|_\sigma = 0 \quad \Rightarrow \quad \dot{\epsilon} = \dot{\gamma}\frac{\partial \phi}{\partial \sigma} \tag{18}$$

$$\frac{\partial L}{\partial \kappa^\star}|_\kappa = 0 \quad \Rightarrow \quad \dot{\lambda} = \dot{\gamma}\frac{\partial \phi}{\partial \kappa} \tag{19}$$

$$\frac{\partial L}{\partial \dot{\gamma}^\star}|_{\dot{\gamma}} = 0 \quad \Rightarrow \quad \frac{\partial \phi}{\partial \dot{\gamma}} = 0 \tag{20}$$

$$\dot{\gamma} \geq 0 \; ; \; \phi \leq 0 \tag{21}$$

The expression of the plastic multiplier $\dot{\gamma}$ can be determined according to the so-called consistency condition (Eqn. 20) which states that, within plastic evolution, the yield criterion remains equal to zero, that is:

$$\dot{\phi} = 0 \quad \Rightarrow \quad \dot{\gamma} = \frac{\frac{\partial \phi}{\partial \sigma} E \dot{\epsilon}}{\frac{\partial \phi}{\partial \sigma} E \frac{\partial \phi}{\partial \sigma} + \frac{\partial \phi}{\partial \kappa} H \frac{\partial \phi}{\partial \kappa}} \geq 0 \tag{22}$$

It is now possible to give the expression of the rate of evolution of sigma and of the tangent modulus $C = \frac{d\sigma}{d\epsilon}$:

$$\dot{\sigma} = E\left(\dot{\epsilon} - \dot{\gamma}\frac{\partial \phi}{\partial \sigma}\right) \quad \Rightarrow \quad C = \begin{cases} E & \text{if } \dot{\gamma} = 0 \text{ (elasticity)} \\ \frac{EH}{E+H} & \text{if } \dot{\gamma} > 0 \text{ (plastic evolution)} \end{cases} \tag{23}$$

According to the position considered in the beam, the yield stress – defined as a lognormal random variable – is allowed to vary, leading to spatial variability in the material behavior law. To illustrate the effect of this variability on the local constitutive response, Fig. 1 presents the local constitutive response at three different points in the beam. Although the yield stress is considered heterogeneous, the loading and unloading slopes remain constant throughout.

4. NUMERICAL APPLICATIONS

4.1. Preliminaries

The fiber element and the constitutive behavior law have been implemented in the finite element computer program FEAP (FEAP 2002). Fibers are defined as a regular mesh of rectangles. Realizations of the lognormal random field $f_0(\mathbf{x})$ are generated using the spectral representation method (Shinozuka & Deodatis 1991) on a regular square grid. The size of each square is equal to one quarter of the correlation length $\ell_c = 1$ cm, which corresponds to approximately half the usual maximum aggregate size. In every element control section, and at every fiber centroid, the random field is, for the sake of simplicity in this preliminary investigation, interpolated by linear polynomial functions.

At every numerical integration point (NIP), classical return-mapping algorithm (Simo & Hughes 1998, Ibrahimbegovic 2009) is applied to update the internal variables, the axial stress and the tangent modulus. Because only linear hardening is considered, no iterative updating procedure is required at the NIP

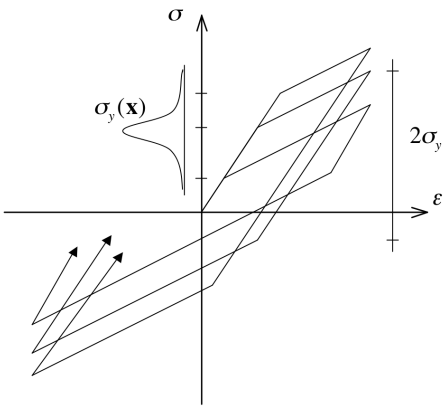

Figure 1: Local elasto-plastic behavior law with linear kinematic hardening. The yield stress varies according to the position in the beam. During elastic loading/unloading, the slope is E; during plastic loading, it is $\frac{EH}{E+H}$.

level, which renders local computation very fast and robust. In the case of dynamic applications, the Newmark method with parameters $\beta = 0.25$ and $\gamma = 0.5$ will be used.

It should be recalled here that no damping model, *e.g.* Rayleigh damping, is used. All the energy dissipation and apparent damping that appear are a consequence of the combination of the simple local elasto-plastic model and of the heterogeneous character of the yield stress.

4.2. Uniaxial force-displacement behavior

We consider a concrete bar of length $L = 2$ m and rectangular section of area $A = 20 \times 30$ cm^2, with right end fixed and imposed displacement at left end. Only one control section is considered. First, we investigate the influence of the variance τ of the random field on the bar response. Figure 2 shows the bar response in cyclic compression for several values of the variance parameter. The curves are plotted with the following set of parameters: $E = 30$ GPa, $H = 10$ GPa, $\sigma_y = 15$ MPa, and $n_{fib} = 20 \times 30$.

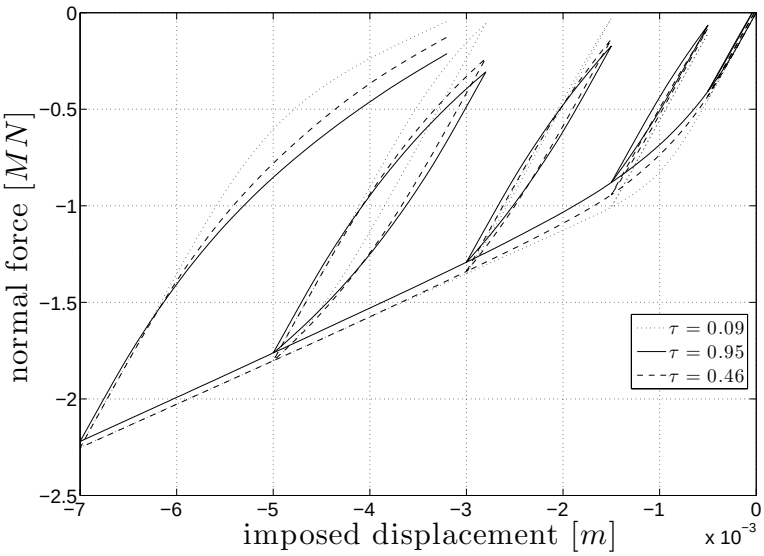

Figure 2: Concrete bar response in cyclic compression for several values of the variance parameter of the lognormal random field. Material constitutive law is elasto-plastic with linear kinematic hardening.

One can observe in Figure 2 that the higher the variance, i) the sooner begins the hardening phase, and ii) the larger are the hysteresis loops during unloading-reloading cycles. Modeling the latter phenomenon would require advanced material constitutive law in the absence of variability (Ragueneau et al. 2000, Jehel et al. 2010) and is a key point to grasp the material contribution to the overall structural damping in earthquake engineering applications. Besides, we recall that the kinematic hardening introduced in the material model is linear and, thus, accounting for spatial variability of the yield stress leads to a smooth structural response that would otherwise only be obtained with a non-linear kinematic hardening model.

Then, we focus on two interrelated issues: How is the bar response dependent i) on the realization $\mathcal{F}_i$ of the random field, and ii) on the number of fibers n_{fib} in the control section? In Table 1, the cumulated plastic energy $\mathcal{E}^p$ dissipated during the compressive cyclic loading is computed for several realizations of the same random field – $\tau = 0.1$ – and for several fiber discretizations. It is shown that, for discretization finer than 20×30 fibers, the cumulated plastic energy $\mathcal{E}^p$ significantly depends neither on the random field realization nor on the fiber discretization.

Table 1: Cumulated plastic energy dissipated during compressive cyclic loading for several realizations of the same random field (lines) and for several fiber sizes (columns).

$[kN.m]$	4×6	6×9	10×15	20×30	30×45	50×75
$\mathcal{F}_1$	5540	5533	5503	5474	5487	5486
$\mathcal{F}_2$	5548	5492	5517	5449	5462	5466
$\mathcal{F}_3$	5355	5478	5464	5459	5468	5468
$\mathcal{F}_4$	5340	5381	5483	5483	5491	5492

Finally, we add a linear softening phase to the elasto-plastic behavior law, as detailed in (Jehel et al. 2010). As first investigation, the ultimate stress $\sigma_u(\mathbf{x})$ before softening begins is modified according to the fluctuations of the same random field as the yield stress $\sigma_y(\mathbf{x})$. Figure 3 shows the response of the bar obtained with the same set of parameters as in Figure 2, and the following additional parameters for linear softening: $K = -5$ GPa and $\sigma_u = 50$ MPa; moreover, the variance is set to $\tau = 0.95$, and $n_{fib} = 20 \times 30$.

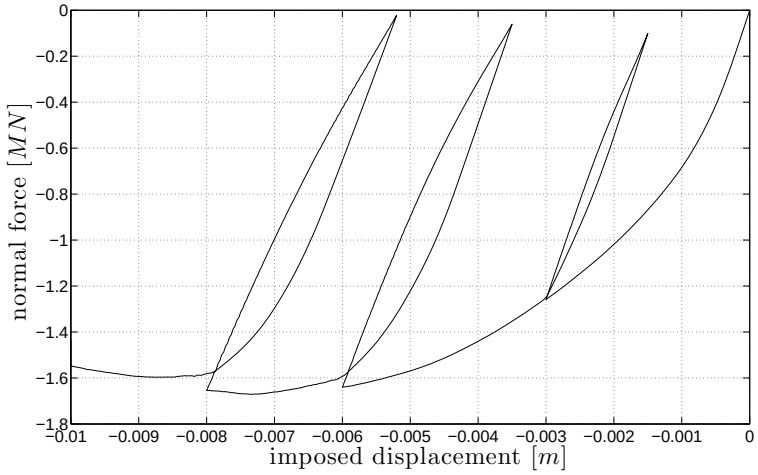

Figure 3: Concrete bar response in cyclic compression when linear softening is added to the elasto-plastic material constitutive law with linear kinematic hardening ($\tau = 0.95$).

In Figure 3, one can see that a nonlinear hardening phase is reproduced by the model, even if the local material response – at every NIP – only is capable of representing linear hardening. Hysteresis loops

are again generated during unloading-reloading cycles. The behavior reproduced here is much more in accordance with the actual behavior of concrete than in Figure 2 (see classical strain-stress concrete experimental response in cyclic compressive loading in Figure 4 (Ramtani 1990)).

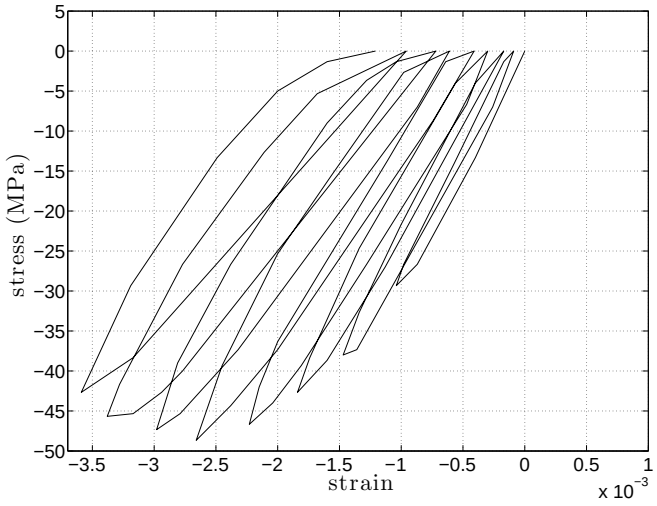

Figure 4: Strain-stress concrete experimental response in pseudo-static cyclic compressive loading.

4.3. Dynamic bending response of a RC cantilever beam

The RC cantilever beam considered here has the same geometry as the bar in the previous experiments, but the boundary conditions are different: the left end is fixed and, at the right end, a constant compressive force of 1 MN is applied within 1 s and, at $t = 1$ s, an impulse force is imposed orthogonally to the beam longitudinal axis $\mathbf{e}_1$, so that the larger moment of inertia is solicited. An additional mass $M = 600$ kg is located at the right end. The fundamental eigenperiod is $T_0 = 0.1$ s. Two control sections, with uncorrelated mechanical properties, are considered along the beam element.

The beam is made of both concrete and four rebars of diameter $\phi = 18$ mm and whose centroid is positioned at 4 cm of the section corners. For concrete, the same set of parameters as in the previous examples is considered, both for the mechanical properties and for the random field. For steel, the elasto-plastic constitutive law with linear kinematic hardening presented in section 3 is used, but without introducing variability and with $E = 200$ GPa, $H = 10$ GPa, and $\sigma_y = 250$ MPa. Each steel rebar is represented by one steel fiber.

Figure 5 shows the displacement time-history of the free end of the cantilever beam for three simulations of the same beam model but with different variance parameter of the lognormal random field describing the spatial variability of $\sigma_y(\mathbf{x})$ and $\sigma_u(\mathbf{x})$. In accordance with the better capability of the concrete behavior law for dissipating energy even for low-amplitude cycles already pointed out for the higher variance in Figure 3, one can see in Figure 5 that almost all the imparted energy is dissipated after 14 s when $\tau = 1.06$. We recall that no damping – *e.g.* Rayleigh damping – has been added in the simulations. This experiment shows that the stochastic constitutive model developed in this paper can represent the structural effects of the material energy dissipation mechanisms.

5. CONCLUSIONS AND ONGOING WORK

For a single-degree-of-freedom elasto-plastic system with linear kinematic hardening, we have shown here two illustrations of the capability of a heterogeneous model of the yield stress to create patterns classically associated to material viscous damping. These patterns would otherwise be modeled through

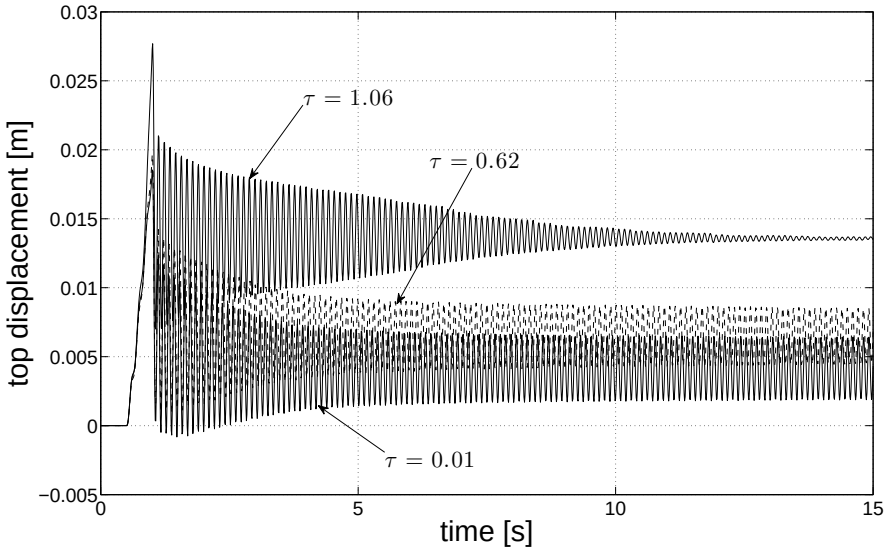

Figure 5: Single DOF RC cantilever beam dynamic response in free vibration: free-end displacement time-history.

either more advanced material constitutive models or additional damping models, *e.g.* Rayleigh damping, lacking physical basis. Although the underlying model for the yield stress is stochastic, the simulations and results are valid for each realization.

The main research prospect after this first illustration lies in the precise characterization of the stochastic model based on the information from the micro-scale (such as aggregate size, granulometry, *etc*.). Indeed, at the scale considered, the variance in particular is some averaged variance of the interpolated random field, which is different from the variance of a corresponding micro-scale random field (Vanmarcke et al. 1986). This will consist in choosing, based on rational arguments, the type of first-order marginal law and correlation model, as well as the value of the corresponding parameters (mean value, variance parameter, and correlation length). This choice and study could be performed in the context of stochastic micro-meso scale transition (Soize 2008, Arnst & Ghanem 2008, Cottereau et al. 2011).

REFERENCES

Arnst, M. and Ghanem, R. (2008). Probabilistic equivalence and stochastic model reduction in multiscale analysis. *Computer Methods in Applied Mechanics and Engineering* **197**, 43–44, 3584–3592.

Benkemoun, N., Hautefeuille, M., Colliat, J.-B. and Ibrahimbegovic, A. (2010). Failure of heterogeneous materials: 3D meso-scale FE models with embedded discontinuities. *International Journal for Numerical Methods in Engineering* **82**, 1671–1688.

Charney, F.A. (2008). Unintended consequences of modeling damping in structures. *Journal of Structural Engineering* **134:4**, 581–592.

Cottereau, R., Clouteau, D. and Soize, C. (2008). Probabilistic impedance of foundation: impact on the seismic design on uncertain soils. *Earthquake Engineering and Structural Dynamics* **37:6**, 899–918.

Cottereau, R., Clouteau, D., Ben Dhia, H., and Zaccardi C. (2011). A stochastic - deterministic coupling method for continuum mechanics. *Computer Methods in Applied Mechanics and Engineering* **207:47-48**, 3280–3288.

FEAP: A Finite Element Analysis Program, User Manual and Programmer Manual, version 7.4. (October 2002). Department of Civil and Environmental Engineering, University of California, Berkeley, CA.

Hall, J.F. (2006). Problems encountered from the use (or misuse) of Rayleigh damping. *Earthquake Engineering and Structural Dynamics* **35**, 525–545.

Hill, R. (1950). The mathematical theory of plasticity. Clarenden Press, Oxford, U.K.

Ibrahimbegovic, A. (2009). Nonlinear Solid Mechanics: Theoretical Formulations and Finite Element Solution Methods. Springer.

Jaynes, E. T. (1957) Information theory and statistical mechanics. *Physical Reviews* **106:4**, 620–630.

Jehel, P., Ibrahimbegovic, A., Léger, P., Davenne, L. (2010). Towards robust viscoelastic-plastic-damage material model with different hardenings / softenings capable of representing salient phenomena in seismic loading applications. *Computers and Concrete* **7:4**, 365–386.

Lee, T.-H. and Mosalam, K.M. (2004). Probabilistic fiber element modeling of reinforced concrete structure. *Computers & Structures* **82**, 2285–2299.

Maugin, G.A. (1999). The thermodynamics of nonlinear irreversible behaviors – An introduction. World Scientific, Singapore.

PEER/ATC-72-1 (October 2010). Modeling and Acceptance Criteria for Seismic Design and Analysis of Tall Buildings, prepared by Applied Technology Council for Pacific Earthquake Engineering Research Center.

Ragueneau, F., La Borderie, C. and Mazars, J. (2000). Damage model for concrete-like materials coupling cracking and friction, contribution towards struc-ural damping: first uniaxial applications. *Mechanics of Cohesive-Frictional Materials* **5**, 607–625.

Ramtani, S. (1990). Contribution to the modeling of the multi-axial behavior of damaged concrete with description of the unilateral characteristics. PhD thesis (in French): Paris 6 University.

Real, M.V., Filho, A.C. and Maestrini, S.R. (2003). Response variability in reinforced concrete structures with uncertain geometrical and material properties. *Nuclear Engineering and Design* **226**, 205–220.

Shannon, C. (1948) A mathematical theory of communication. *Bell Systems Technological Journal* **27:3**, 379–423.

Shinozuka, M. and Deodatis, G. (1991) Simulation of stochastic processes by spectral representation. *Applied Mechanics Reviews* **44:4**, 191–203.

Simo, J.C. and Hughes, T.J.R. (1998). Computational Inelasticity, Springer, Berlin.

Soize, C. (2006). Non-Gaussian positive-definite matrix-valued random fields for elliptic stochastic partial differential operators. *Computer Methods in Applied Mechanics and Engineering* **195:1-3**, 26–64.

Soize, C. (2008). Tensor-valued random field for meso-scale stochastic model of anisotropic elastic microstructure and probabilistic analysis of representative volume element size. *Probabilistic Engineering Mechanics* **23:2-3**, 307–323.

Stefanou, G. and Fragiadakis, M. (2009). Nonlinear dynamic analysis of frames with stochastic non-Gaussian material properties. *Engineering Structures* **31**, 1841–1850.

Strang, G. (1986). Introduction to Applied Mathematics, Wellesley Cambridge Press, Wellesley, MA.

Ta, Q.-A., Clouteau, D. and Cottereau, R. (2010). Modeling of random anisotropic elastic media and impact on wave propagation. *European Journal of Computational Mechanics* **19:1-3**, 241–253.

Taylor, R.L., Filippou, F.C., Saritas, A. and Auricchio, F. (2003). A mixed finite element method for beam and frame problems. *Computational Mechanics* **31**, 192–203.

Vanmarcke, E., Shinozuka, M., Nakagiri, S., Schueller, G.I. and Grigoriu, M. (1986). Random fields and stochastic finite elements. *Structural Safety* **3**, 143–166.